ACS OMEGA

http://pubs.acs.org/journal/acsodf

Article

Evaluation of Effective Field-Effect Mobility in Thin-Film and Single-Crystal Transistors for Revisiting Various Phenacene-Type Molecules

Yanting Zhang, Ritsuko Eguchi, Shino Hamao, Hideki Okamoto, Hidenori Goto, and Yoshihiro Kubozono*

Cite This: *ACS Omega* 2022, 7, 5495−5501

Read Online

ACCESS | Metrics & More | Article Recommendations

ABSTRACT: The magnitude of the field-effect mobility μ of organic thin-film and single-crystal field-effect transistors (FETs) has been overestimated in certain recent studies. These reports set alarm bells ringing in the research field of organic electronics. Herein, we report a precise evaluation of the μ values using the effective field-effect mobility, μ_{eff}, a new indicator that is recently designed to prevent the FET performance of thin-film and single-crystal FETs based on various phenacene molecules from being overestimated. The transfer curves of a range of FETs based on phenacene are carefully categorized on the basis of a previous report. The exact evaluation of the value of μ_{eff} depends on the exact classification of each transfer curve. The transfer curves of all our phenacene FETs could be successfully classified based on the method indicated in the aforementioned report, which made it possible to evaluate the exact value of μ_{eff} for each FET. The FET performance based on the values of μ_{eff} obtained in this study is discussed in detail. In particular, the μ_{eff} values of single-crystal FETs are almost consistent with the μ values that were reported previously, but the μ_{eff} values of thin-film FETs were much lower than those previously reported for μ, owing to a high absolute threshold voltage, $|V_{th}|$. The increase in the field-effect mobility as a function of the number of benzene rings, which was previously demonstrated based on the μ values of single-crystal FETs with phenacene molecules, is well reproduced from the μ_{eff} values. The FET performance is discussed based on the newly evaluated μ_{eff} values, and the future prospects of using phenacene molecules in FET devices are demonstrated.

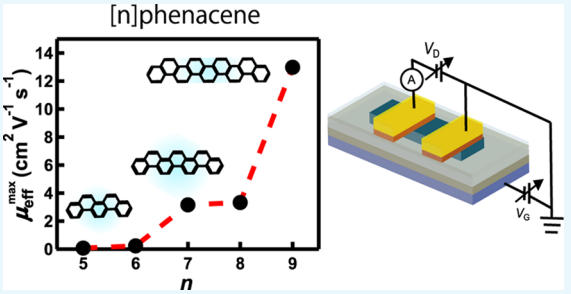

1. INTRODUCTION

Studies that have highlighted the overestimation of the magnitude of the field-effect mobility, μ, in organic field-effect transistors (FETs) have recently been reported,[1,2] which set the alarm bells ringing in the research field of organic electronics.[1,2] The development of organic FETs during the past decade has led to rapid enhancements in μ, but the abovementioned reports indicate that these very high μ values might be apparent values. Namely, the value of μ might not be an appropriate indicator for evaluating the FET properties[2] if the μ values are determined from the steepest slope of the transfer curves.

It should be noted that the exact channel mobility, which does not include the contact resistance, must be evaluated in a four-terminal mode.[3−5] Conceivably, the transmission line method (TLM) has been effectively employed to evaluate the contact resistance.[6−8] Moreover, many attempts to directly reduce the contact resistance have been reported, such as matching the work function, ϕ, of metals for source/drain electrodes with the energy levels of the conduction or valence bands[9−11] and inserting various electron acceptor molecules between the electrodes and active layers.[12−14] Thus, the μ value determined in the two-terminal mode has been predicted to underestimate the channel mobility owing to the contact resistance.[3−5] In this regard, it is important to note that the recently reported high μ values were measured in the two-terminal mode,[15−17] which may originate from the advancement of material design. However, a significant claim was made that the value of μ would not become a suitable indicator for the FET operation if the transfer curves were not evaluated appropriately.[1,2] Thus, the μ value determined simply from the steepest slope of the transfer curve was no longer considered to be an indicator of the FET performance owing to the overestimation of this value.[2] This prompted the design of the effective field-effect mobility, μ_{eff}, as a new indicator of FET performance to avoid the overestimation of μ. The μ_{eff} value corresponds to the field-effect mobility evaluated by reconstructing the transfer curve obtained experimentally to the ideal Shockley type. The value of μ_{eff} drastically differs from

Received: December 7, 2021
Accepted: January 12, 2022
Published: January 31, 2022

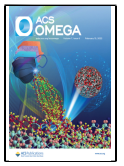

https://doi.org/10.1021/acsomega.1c06932
ACS Omega 2022, 7, 5495−5501

that of μ depending on the type of transfer curve.[2] Therefore, the value of μ_{eff} in organic FETs has to be determined by exactly classifying the transfer curves.

Herein, we report the evaluation of μ_{eff} of FETs using both single crystals and thin films of phenacene molecules with the aim of clarifying their real FET performance. High μ values have been reported for FETs with phenacene molecules,[5,7,12−14,16,18−28] and an increase in the μ value using an extension of the benzene network has also been demonstrated.[18,20] In addition to these results, the potential application of phenacene molecules in future practical FET devices owing to their higher stability than acene molecules under atmospheric conditions is considered. However, a re-evaluation of the FET properties of phenacene molecules using the new indicator, μ_{eff}, is necessary because of the significant claim mentioned above. The purpose of this study is to summarize the FET properties of phenacene molecules based on the μ_{eff} values and to demonstrate the availability of these molecules for FET applications. Therefore, we strictly followed the concept and idea of μ_{eff} proposed in ref 2 to exactly evaluate the performance of phenacene FETs. The molecular structures of all molecules employed in this study are shown in Figure 1, which are categorized "phenacene molecules".

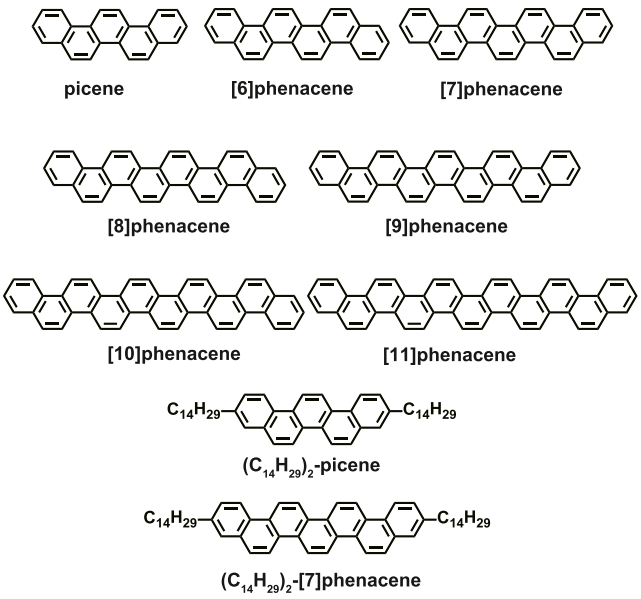

Figure 1. Molecular structures of phenacene molecules employed in this study.

2. METHODS

The μ_{eff} values of FETs based on both single crystals and thin films of phenacene molecules were determined according to the previously described method.[2] All FET data were taken from our own studies.[5,12−14,16,18−25,27,28] Each transfer curve was first classified as belonging to one of the six types, as reported before.[2] These six types of transfer curves are categorized as "model A−F," as shown in Figure 2. The measurement reliability factor, r_{sat}, for the saturation regime was evaluated using the following formula[2]

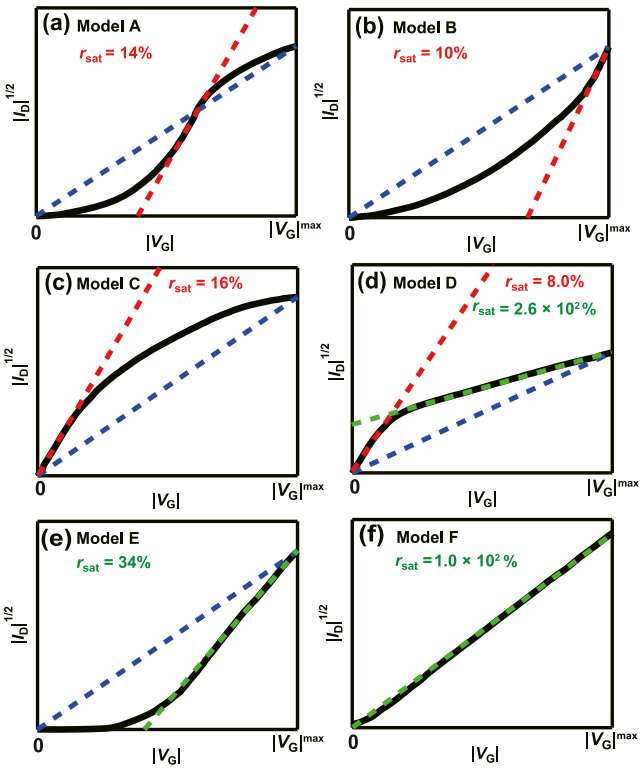

Figure 2. Simulated transfer characteristics classified as model A−F. (a) An S-shaped transfer curve, (b) superlinear curve, (c) sublinear curve, and (d) humped nonlinear curve. (e) Linear characteristics with high $|V_{th}|$ and (f) ideal Shockley-type transfer curve. The meaning of the dashed lines is described in detail in the text. The values of r_{sat} were evaluated based on the formulae shown in the text.

$$r_{sat} = \left(\frac{\sqrt{|I_D|^{max}} - \sqrt{|I_D|^0}}{|V_G|^{max}} \right)^2 \Big/ \left(\frac{WC_i}{2L} \mu_{sat} \right)$$

$$= \left(\frac{\sqrt{|I_D|^{max}} - \sqrt{|I_D|^0}}{|V_G|^{max}} \right)^2 \Big/ \left(\frac{\partial \sqrt{|I_D|}}{\partial |V_G|} \right)^2$$

where μ_{sat}, L, W, and C_i refer to the field-effect mobility μ evaluated in the saturation regime, channel length, channel width, and capacitance per area of the gate dielectric, respectively. $|I_D|^{max}$ and $|I_D|^0$ are the experimental maximum absolute drain current and the experimental absolute drain current at a gate voltage V_G of 0 V, respectively, and the drain current is I_D. $\frac{\partial \sqrt{|I_D|}}{\partial |V_G|}$ corresponds to the slope of the plot of $\sqrt{|I_D|}$ against $|V_G|$, in which μ_{sat} was evaluated and $\frac{\partial \sqrt{|I_D|}}{\partial |V_G|}$ generally refers to the steepest slope. The value of μ_{eff} was evaluated using the formula,[2] $\mu_{eff} = r_{sat} \times \mu_{sat}$. Namely, in the case of an ideal Shockley-type transfer curve displayed as model F (Figure 2), r_{sat} = 100%.[2] Throughout this study, μ_{sat} is simply denoted "μ."

Moreover, we evaluated the measurement reliability factor r_{lin} and effective field-effect mobility μ_{eff}^{lin} from the field-effect mobility μ_{lin} in the linear regime, determined for [6]phenacene thin-film FET.[5] Here, the value of r_{lin} was estimated using the following formula[2]

https://doi.org/10.1021/acsomega.1c06932
ACS Omega 2022, 7, 5495−5501

$$r_{lin} = \left(\frac{|I_D|^{max} - |I_D|^0}{|V_G|^{max}}\right) / \left(\frac{|V_D| W C_i}{L} \mu_{lin}\right)$$
$$= \left(\frac{|I_D|^{max} - |I_D|^0}{|V_G|^{max}}\right) / \frac{\partial |I_D|}{\partial |V_G|}$$

Moreover, $\mu_{eff}^{lin} = r_{lin} \times \mu_{lin}$.

3. RESULTS AND DISCUSSION

Figure 2 shows a schematic drawing of the six types of transfer curves, $|I_D|^{1/2}$ versus $|V_G|$, of organic FETs in the saturation regime. These transfer curves are categorized as "model A−F"; the value of r_{sat} shown in Figure 2 varies largely across these six models. The schematically drawn transfer curves (Figure 2) are based on the description in the previous report.[2] The ideal transfer curve refers to that categorized as "model F" for which r_{sat} is ∼100%. The transfer curve for model F, characterized by a small absolute threshold voltage $|V_{th}|$ (∼0), implies an ideal Shockley-type transfer curve. In contrast, model A has an S-shaped transfer curve (Figure 2a). The value of μ for model A is determined from the part of the transfer curve with the steepest slope (red-dashed line) and r_{sat} is 14%. Model B (Figure 2b) displays a superlinear curve, where $|V_{th}|$ is too high, and r_{sat} is 10%. Model C (Figure 2c) has a sublinear curve, and r_{sat} is 16%. The values of r_{sat} in models A−C are unacceptably low. The transfer curves of the two remaining models, D and E, are nonlinear with a hump in the subthreshold region with an extended linear characteristic (model D) and a linear characteristic with high $|V_{th}|$ (model E), as shown in Figure 2d,e, respectively. The values of r_{sat} were 8 and 34% for models D and E, respectively. Here, an r_{sat} value of 8% (model D) was evaluated from the red line in Figure 2d. For model D, the green-dashed line may be selected, as shown in Figure 2d. In this case, the dashed line does not refer to the steepest part of the transfer curve, but to the moderately steep part; in this case, r_{sat} is 260%, indicating that μ is underestimated.

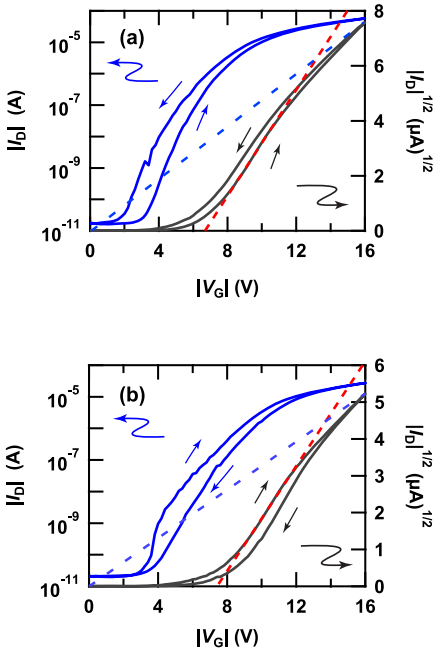

Figure 3. Transfer curves of 3,10-ditetradecylpicene ($(C_{14}H_{29})_2$-picene) thin-film FETs with (a) PZT and (b) ZrO_2 gate dielectrics. Only the values of μ, $|V_{th}|$, the on−off ratio, and S of these devices are reported in ref 16, but the transfer curves were not shown previously.

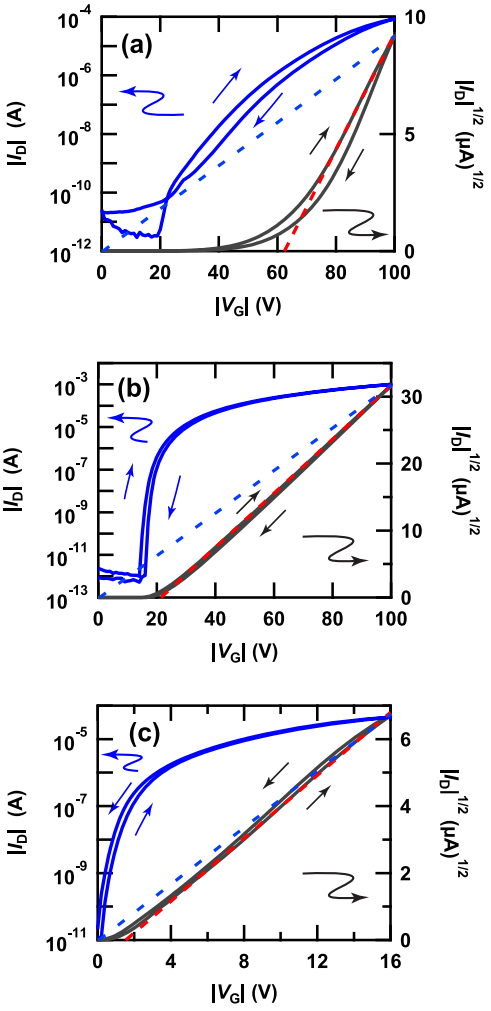

Figure 4. Transfer curves of (a) [6]phenacene thin-film FET with SiO_2 gate dielectric. Transfer curves of [9]phenacene single-crystal FET with (b) SiO_2 and (c) PZT gate dielectrics. Only the values of μ, $|V_{th}|$, the on−off ratio, and S of these devices were reported in refs 5 and 20, but the transfer curves were not shown previously.

By definition, r_{sat} is an indicator of the deviation from the ideal transfer curve (model F). The values of r_{sat} in models A−E (Figure 2a−e) are smaller than those in the ideal transfer curve (model F), leading to an overestimation of the field-effect mobility; the red line is selected in model D (Figure 2d). As described above, r_{sat} may increase by selecting the extended linear part (green-dotted line) for the evaluation of the μ value in model D, as shown in Figure 2d, which results in the field-effect mobility being underestimated. In fact, the transfer curves of models A−E result in an overestimation of μ, because the value of μ is generally determined from the steepest part of the transfer curve. The key to obtaining the ideal transfer curve is to suppress the value of $|V_{th}|$. However, certain FETs based on phenacene have a high $|V_{th}|$ value, particularly in the case of a SiO_2 gate dielectric.[5,12−14,16,18−23,25,27,28] This may be the most serious problem associated with the utilization of phenacene molecules as the active layer in FET devices.

Figure 3a,b shows the transfer curves of thin-film FETs based on 3,10-ditetradecylpicene ($(C_{14}H_{29})_2$-picene) with $Pb(Zr,Ti)O_3$ (PZT) and ZrO_2 gate dielectrics. These transfer

https://doi.org/10.1021/acsomega.1c06932
ACS Omega 2022, 7, 5495−5501

Table 1. Parameters of FET Devices Using Thin Films of Phenacene Molecules

sample name	no.	gate dielectric	C_i (nF cm^{-2})	type	$\lvert V_{th}\rvert$ (V)	μ (cm^2 V^{-1} s^{-1})	r_{sat} (%)	μ_{eff} (cm^2 V^{-1} s^{-1})	ref.
picene	1	SiO_2	8.6	B	67	1.1×10^{-1}	10	1.1×10^{-2}	21
	2	SiO_2	8.6	A	60	1.4	22	3.1×10^{-1}	22
	3	ZrO_2	1.4×10^2	B	6.7	3.6×10^{-2}	11	3.9×10^{-3}	24
	4	HfO_2	83	B	6.9	1.5×10^{-2}	9.6	1.4×10^{-3}	
	5	BST	1.0×10^2	B	4.0	1.9×10^{-3}	11	2.1×10^{-4}	
[6]phenacene	6	SiO_2	11	B	62	3.7	14	5.3×10^{-1}	25
	7	Ta_2O_5	64	B	5.4	9.0×10^{-2}	21	1.9×10^{-2}	
	8	SiO_2	8.1	B	69	7.4	9.4	7.0×10^{-1}	5
	9[a]	SiO_2	8.1	B	62	6.6	14	9.2×10^{-1}	
	10	Parylene	3.0	B	100	6.0×10^{-1}	7.5	4.5×10^{-2}	
	11	Parylene	3.0	B	100	4.6×10^{-1}	8.4	3.9×10^{-2}	
	12	parylene	3.0	B	86	5.7×10^{-2}	8.0	4.5×10^{-3}	
	13	parylene	3.8	B	56	2.7	23	6.1×10^{-1}	
[7]phenacene	14	SiO_2	8.1	B	55	8.4×10^{-1}	20	1.7×10^{-1}	23
	15	HfO_2	83	B	4.5	1.6×10^{-2}	13	2.0×10^{-3}	
	16	BMIM-PF_6	9.7×10^3	B	2.7	2.6×10^{-1}	1.0	2.6×10^{-3}	
	17	EMIM-TFSI	9.3×10^3	E	1.7	1.0×10^{-3}	10	1.0×10^{-4}	
	18	BMIM-PF_6	9.7×10^3	B	2.5	2.8×10^{-1}	2.8	7.8×10^{-3}	
	19	SiO_2	8.3	B	66	9.2×10^{-1}	12	1.1×10^{-1}	27
[8]phenacene	20	SiO_2	8.1	B	51	1.7	24	4.1×10^{-1}	19
	21	BMIM-PF_6	4.0×10^3	E	2.7	16	8.0×10^{-1}	1.3×10^{-1}	
[9]phenacene	22	SiO_2	8.3	B	49	1.5×10^{-1}	26	3.8×10^{-2}	20
	23	SiO_2	8.3	B	42	1.7	32	5.4×10^{-1}	
[10]phenacene	24	SiO_2	8.3	B	39	3.7×10^{-2}	37	1.4×10^{-2}	28
	25	BMIM-PF_6	8.0×10^3	A	2.2	4.2	1.4	5.7×10^{-2}	
[11]phenacene	26	SiO_2	8.3	B	43	1.2×10^{-1}	19	2.2×10^{-2}	28
	27	BMIM-PF_6	8.0×10^3	E	2.3	2.6	1.1	2.8×10^{-2}	
$(C_{14}H_{29})_2$-picene	28	SiO_2	8.3	B	51	3.9	13	5.1×10^{-1}	16
	29	HfO_2	35	A	11	7.7	18	1.4	
	30[b]	PZT	36	A	6.7	13	24	3.1	
	31	PZT	36	A	9.8	13	14	1.8	
	32[c]	ZrO_2	35	A	7.6	8.9	18	1.6	
$(C_{14}H_{29})_2$-[7]phenacene	33	SiO_2	8.3	E	25	2.0	56	1.1	27
	34	ZrO_2	39	E	6.4	2.2×10^{-1}	37	7.9×10^{-2}	
	35	BMIM-PF_6	8.0×10^3	A	2.4	1.3	2.5	3.1×10^{-2}	

[a]The transfer curve of the device (no. 9) is shown in Figure 4a. [b]The transfer curve of the device (no. 30) is shown in Figure 3a. [c]The transfer curve of the device (no. 32) is shown in Figure 3b.

curves, which provide high values of μ of 13 and 8.9 cm^2 V^{-1} s^{-1}, respectively, as reported previously,[16] are categorized as model A. The values of r_{sat} for these transfer curves were 24 and 18%, respectively. Consequently, the values of μ_{eff} were estimated to be 3.1 and 1.6 cm^2 V^{-1} s^{-1}, respectively, for $(C_{14}H_{29})_2$-picene thin-film FETs with PZT and ZrO_2 gate dielectrics, indicating that the mobility is still high. In particular, the FET performance of the $(C_{14}H_{29})_2$-picene thin-film FET (μ_{eff} = 1.4−3.1 cm^2 V^{-1} s^{-1}) with high-k gate dielectrics is highly attractive, even though the effective mobility was employed for the evaluation of the FET performance. The $\lvert V_{th}\rvert$ values for the $(C_{14}H_{29})_2$-picene thin-film FETs with PZT and ZrO_2 gate dielectrics were 6.7 and 7.6 V, respectively, suggestive of low-voltage operation. Thus, the results suggest that $(C_{14}H_{29})_2$-picene is a highly suitable material for the active layer (thin film) of FET devices when using high-k gate dielectrics.

The transfer curve of the [6]phenacene thin-film FET with a SiO_2 gate dielectric is shown in Figure 4a, and is categorized as model B, characterized by a superlinear curve. The value of r_{sat} from the transfer curve shown in Figure 4a is 14%. Namely, the very high $\lvert V_{th}\rvert$ of 62 V causes a large deviation from the ideal Shockley-type transfer curve (model F). Based on the value of μ (= 6.6 cm^2 V^{-1} s^{-1})[5] for [6]phenacene thin-film FETs with SiO_2 gate dielectrics, the value of μ_{eff} was estimated to be 9.2×10^{-1} cm^2 V^{-1} s^{-1}. Thus, the value of μ_{eff} was reduced by the large deviation from the ideal transfer curve.

The transfer curve of the [9]phenacene single-crystal FET with a SiO_2 gate dielectric is shown in Figure 4b, and is categorized as model E. This type of transfer curve is characterized by a linear characteristic with a high $\lvert V_{th}\rvert$. In fact, $\lvert V_{th}\rvert$ is 22 V, that is, the transfer curve closely approximates the ideal type (model F). The value of r_{sat} derived from the transfer curves shown in Figure 4b is 61%. The value of μ_{eff} was estimated to be 5.3 cm^2 V^{-1} s^{-1} from the value of μ (=8.7 cm^2 V^{-1} s^{-1})[20] for the [9]phenacene single-crystal FET with SiO_2, indicating a high field-effect mobility. The transfer curve shown in Figure 4c is that of the [9]phenacene single-crystal FET with a PZT gate dielectric. This curve yields the values of 81% and 4.5 cm^2 V^{-1} s^{-1} for r_{sat} and μ_{eff}, respectively, and is also categorized as model A. Thus, [9]phenacene single-crystal FETs have transfer curves of which the shape is close to that of the ideal Shockley-type transfer curve (model F).

https://doi.org/10.1021/acsomega.1c06932
ACS Omega 2022, 7, 5495−5501

Table 2. Parameters of FET Devices Using Single Crystals of Phenacene Molecules

sample name	no.	gate dielectric	C_i (nF cm^{-2})	type	$\lvert V_{th}\rvert$ (V)	μ (cm^2 V^{-1} s^{-1})	r_{sat} (%)	μ_{eff} (cm^2 V^{-1} s^{-1})	ref.
Picene	1	SiO_2	6.8	B	96	4.7×10^{-1}	13	6.3×10^{-2}	12
	2	SiO_2	32	B	30	8.6×10^{-2}	8.2	7.1×10^{-3}	
	3	Ta_2O_5	28	E	26	3.4×10^{-2}	4.9	1.7×10^{-3}	
	4	Ta_2O_5	28	B	27	4.0×10^{-1}	5.1	2.0×10^{-2}	
	5	HfO_2	26	E	30	1.1	6.3	6.9×10^{-2}	
	6	BMIM-PF_6	9.6×10^3	A	1.9	1.8×10^{-1}	1.9	3.4×10^{-3}	
[6]phenacene	7	SiO_2	9.1	E	36	5.6×10^{-1}	41	2.3×10^{-1}	13
[7]phenacene	8	SiO_2	9.1	B	91	2.6×10^{-2}	5.8	1.5×10^{-3}	13
	9	SiO_2	9.1	E	54	2.3	30	7.0×10^{-1}	
	10	HfO_2	49	E	2.6	3.0	76	2.3	
	11	SiO_2	9.1	E	18	4.7	67	3.2	
	12	Ta_2O_5	49	E	6.3	3.2	47	1.5	
	13	BMIM-PF_6	9.7×10^3	E	2.3	3.8×10^{-1}	5.4	2.1×10^{-2}	
	14	SiO_2	11	E	50	6.9	34	2.3	14
[8]phenacene	15	SiO_2	10	E	28	8.2	41	3.3	18
	16	PZT	63	E	4.9	2.1	48	1.0	
	17	BMIM-PF_6	7.9×10^3	B	2.4	3.5×10^{-1}	4.8	1.7×10^{-2}	
[9]phenacene	18	SiO_2	9.5	E	17	10.5	70	7.4	20
	19[a]	SiO_2	9.5	E	22	8.7	61	5.3	
	20	ZrO_2	28	E	2.1	18	72	13	
	21	ZrO_2	28	A	1.3	10	23	2.3	
	22	PZT	41	A	1.4	6.2	76	4.7	
	23	PZT	41	A	1.0	4.6	70	3.2	
	24[b]	PZT	41	A	1.5	5.6	81	4.5	

[a]The transfer curve of the device (no. 19) is shown in Figure 4b. [b]The transfer curve of the device (no. 24) is shown in Figure 4c.

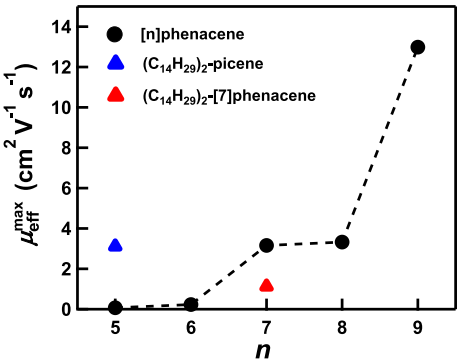

Figure 5. Plot of μ_{eff}^{max} vs n of the phenacene molecules (closed circles). Plots of μ_{eff}^{max} against n for $(C_{14}H_{29})_2$-[n]phenacene thin-film FETs.

Here, we comment on the category to which the 35 transfer curves of thin-film FETs and 24 single-crystal FETs based on phenacenes belong, as summarized in Tables 1 and 2. As seen in Table 1, 66% of thin-film FETs are categorized as model B, which is characterized by a superlinear curve with very high $\lvert V_{th}\rvert$ values, whereas 20% of FETs are categorized as model A, and the remainder as model E. Namely, the transfer curves of most of the phenacene thin-film FETs are categorized as model B because of their high $\lvert V_{th}\rvert$ originating from large gap energy and large trap density. In particular, the low-k gate dielectric like SiO_2 provides a high $\lvert V_{th}\rvert$ to lead to the B-type transfer curve. Thus, the capacitance of the gate dielectric is one of the most important factors to determine the transfer curve, that is, the small capacitance (low-k gate dielectric) requires a larger gate voltage to fill the trap density.

On the other hand, in the case of single-crystal FETs (Table 2), 58% of FETs are categorized as model E, whereas 21% of FETs are categorized as model B, and the remaining FETs as model A. Thus, r_{sat} of single crystal FETs categorized as model E could be divided into two groups: one group with high r_{sat} because of the low $\lvert V_{th}\rvert$, and the other group with low r_{sat} because of the higher $\lvert V_{th}\rvert$. In the case of phenacene single-crystal FETs, the fraction of B-type transfer curves is lower than that of thin-film FETs, demonstrating the trap density of single crystal must be smaller than that of the thin film. Therefore, the B-type transfer curves had not often to be observed.

The contact resistance often led to the concave output curves in organic FETs, but most of the output curves did not provide a remarkable concave behavior in phenacene thin-film FETs, because of the top-contact source/drain electrodes and the insertion of 2,3,5,6-tetrafluoro-7,7,8,8-tetracyanoquinodimethane between the electrodes and active layer. Therefore, the B-type transfer curve owing to the high $\lvert V_{th}\rvert$ of phenacene FETs may not directly be due to the contact resistance.

In addition, as seen from Tables 1 and 2, some FETs with the same structure show the different types of transfer curves, although most of the same structured FETs provided the same ones. This implies that the slight difference of capacitance and coating of the gate dielectric surface may lead to the different types of transfer curves (A, B, and E) even in the same device structure because smaller capacitance and larger trap density provide a B-type transfer curve, and a more rough surface of gate dielectric may provide A-type (suppression of $\lvert I_D\rvert$ at high $\lvert V_G\rvert$) owing to the surface effect.[29]

As shown in Table 2, [8]phenacene and [9]phenacene single-crystal FETs had high r_{sat} values, leading to high values of μ_{eff}, thereby demonstrating that extended phenacene molecules are highly suitable for use as the active layer in FET devices. In the case of [8]phenacene and [9]phenacene single-crystal FETs, the use of SiO_2 as the gate dielectric as

https://doi.org/10.1021/acsomega.1c06932
ACS Omega 2022, 7, 5495−5501

well as high-k gate dielectrics also yields high values of r_{sat} and μ_{eff}. In addition, the [7]phenacene single crystal FETs with high-k gate dielectrics provided high values of r_{sat} and μ_{eff}. Namely, the use of a high-k gate dielectric in [8]phenacene and [9]phenacene single-crystal FETs is not strictly necessary, although [7]phenacene requires it.

We briefly comment on the FET properties of electric-double-layer (EDL) thin-film transistors with ionic liquids, BMIM[PF_6] and EMIM-TFSI, which provide very low values of r_{sat} (less than 11%) as listed in Table 1. The values of μ_{eff} obtained are too low because of the low values of r_{sat}. The trend is also found in single-crystal FETs, as seen from Table 2. Thus, the low μ_{eff} values in EDL thin-film and single-crystal FETs indicate that the phenacene molecules may not be employed for EDL FETs at the present stage.

Figure 5 shows a plot of μ_{eff} versus the number of benzene rings (n) in the phenacene molecules. In the graph, the highest μ_{eff} value (μ_{eff}^{max}) recorded for the FETs using each [n]phenacene is plotted as a function of n, unambiguously demonstrating that the extension of the benzene network in the phenacene molecule is a significant key to improving the FET performance. This is consistent with the results reported previously based on the plot of μ versus n.[18,20] In particular, [9]phenacene is expected to be an excellent molecule for the active layer of single-crystal FETs. Moreover, certain $(C_{14}H_{29})_2$-picene and $(C_{14}H_{29})_2$-[7]phenacene thin-film FETs often have μ_{eff} values higher than 1.0 $cm^2\ V^{-1}\ s^{-1}$, although the transfer curves are classified as models A and B, indicating that alkyl-substituted picene and [7]phenacene molecules are effective for thin-film FETs.

Finally, we evaluated the values of r_{lin} and μ_{eff}^{lin} for [6]phenacene thin-film FET with 400 nm thick SiO_2. The transfer curve was categorized as "model B", as seen from the transfer curve shown in ref 5. The value of r_{lin} was evaluated to be 19%, which gave a value of $\mu_{eff}^{lin} = 7.4 \times 10^{-1}\ cm^2\ V^{-1}\ s^{-1}$ because $\mu_{lin} = 3.9\ cm^2\ V^{-1}\ s^{-1}$.[5] The values are similar to r_{sat} (=14%) and μ_{eff}^{sat} ($=9.2 \times 10^{-1}\ cm^2\ V^{-1}\ s^{-1}$) obtained for the corresponding FET (Figure 4a and Table 1), demonstrating the validity of effective field-effect mobility as an indicator of FET performance.

4. CONCLUSIONS

In conclusion, the transfer curves reported for phenacene molecules were classified into six models based on their characteristics, and the values of r_{sat} and μ_{eff} were evaluated to judge their FET performance correctly. As a result, it was demonstrated that the extension of the benzene network of the phenacene molecules was significant for improving the performance of single-crystal FETs. Specifically, the use of [8]phenacene and [9]phenacene molecules as the active layer showed great potential for improving the performance of single-crystal FETs. Also, [7]phenacene single crystals have potential for FET application in the case of using a high-k gate dielectric. Moreover, alkyl-substituted picene is promising for use as an active layer in thin-film FETs in high-k dielectrics. These results clearly indicate that the extension of the benzene network of the phenacene molecule plays an important role in the improvement of FET performance. We successfully synthesized [10]phenacene and [11]phenacene to fabricate thin-film FETs,[28] but single-crystal FETs have not yet been fabricated using these molecules. This is the most significant task for realizing high-performance single-crystal FETs. Moreover, a suitable design involving the alkyl substitution of [n]phenacenes would be an effective approach to realize high-performance organic thin-film FETs.

AUTHOR INFORMATION

Corresponding Author

Yoshihiro Kubozono − *Research Institute for Interdisciplinary Science, Okayama University, Okayama 700-8530, Japan;* orcid.org/0000-0002-7910-0308; Email: kubozono@cc.oakayama-u.ac.jp

Authors

Yanting Zhang − *Research Institute for Interdisciplinary Science, Okayama University, Okayama 700-8530, Japan*

Ritsuko Eguchi − *Research Institute for Interdisciplinary Science, Okayama University, Okayama 700-8530, Japan*

Shino Hamao − *Research Institute for Interdisciplinary Science, Okayama University, Okayama 700-8530, Japan*

Hideki Okamoto − *Department of Chemistry, Okayama University, Okayama 700-8530, Japan;* orcid.org/0000-0002-8742-4089

Hidenori Goto − *Research Institute for Interdisciplinary Science, Okayama University, Okayama 700-8530, Japan*

Complete contact information is available at: https://pubs.acs.org/10.1021/acsomega.1c06932

Notes

The authors declare no competing financial interest.

ACKNOWLEDGMENTS

This study was partly supported by Grants-in-Aid (19H02676, 20K05648, 20H05878, and 20H05879) from MEXT.

REFERENCES

(1) Bittle, E. G.; Basham, J. I.; Jackson, T. N.; Jurchescu, O. D.; Gundlach, D. J. Mobility overestimation due to gated contacts in organic field-effect transistors. *Nat. Commun.* **2016**, *7*, 10908.

(2) Choi, H. H.; Cho, K.; Frisbie, C. D.; Sirringhaus, H.; Podzorov, V. Critical assessment of charge mobility extraction in FETs. *Nat. Mater.* **2018**, *17*, 2−7.

(3) Goldmann, C.; Haas, S.; Krellner, C.; Pernstich, K. P.; Gundlach, D. J.; Batlogg, B. Hole mobility in organic single crystals measured by a "flip-crystal" field-effect technique. *J. Appl. Phys.* **2004**, *96*, 2080−2086.

(4) Okada, Y.; Sakai, K.; Uemura, T.; Nakazawa, Y.; Takeya, J. Charge transport and Hall effect in rubrene single-crystal transistors under high pressure. *Phys. Rev. B: Condens. Matter Mater. Phys.* **2011**, *84*, 245308.

(5) Eguchi, R.; He, X.; Hamao, S.; Goto, H.; Okamoto, H.; Gohda, S.; Sato, K.; Kubozono, Y. Fabrication of high performance/highly functional field-effect transistor devices based on [6]phenacene thin films. *Phys. Chem. Chem. Phys.* **2013**, *15*, 20611−20617.

(6) Gundlach, D. J.; Zhou, L.; Nichols, J. A.; Jackson, T. N.; Necliudov, P. V.; Shur, M. S. An experimental study of contact effects in organic thin film transistors. *J. Appl. Phys.* **2006**, *100*, 024509.

(7) Sugawara, Y.; Kaji, Y.; Ogawa, K.; Eguchi, R.; Oikawa, S.; Gohda, H.; Fujiwara, A.; Kubozono, Y. Characteristics of field-effect transistors using the one-dimensional extended hydrocarbon [7]-phenacene. *Appl. Phys. Lett.* **2011**, *98*, 013303.

(8) Yang, J.-G.; Seah, W.-L.; Guo, H.; Tan, J.-K.; Zhou, M.; Matsubara, R.; Nakamura, M.; Png, R.-Q.; Ho, P. K. H.; Chua, L.-L. Characterization of ohmic contacts in polymer organic field-effect transistors. *Org. Electron.* **2016**, *37*, 491−497.

(9) Ahles, M.; Schmechel, R.; von Seggern, H. n-type organic field-effect transistor based on interface-doped pentacene. *Appl. Phys. Lett.* **2004**, *85*, 4499−4501.

https://doi.org/10.1021/acsomega.1c06932
ACS Omega 2022, 7, 5495−5501

(10) Ochi, K.; Nagano, T.; Ohta, T.; Nouchi, R.; Kubozono, Y.; Matsuoka, Y.; Shikoh, E.; Fujiwara, A. Output properties of C60 field-effect transistor device with Eu source/drain electrodes. *Appl. Phys. Lett.* **2006**, *89*, 083511.
(11) Takahashi, N.; Maeda, A.; Uno, K.; Shikoh, E.; Yamamoto, Y.; Hori, H.; Kubozono, Y.; Fujiwara, A. Output properties of C60 field-effect transistors with different source/drain electrodes. *Appl. Phys. Lett.* **2007**, *90*, 083503.
(12) Kawai, N.; Eguchi, R.; Goto, H.; Akaike, K.; Kaji, Y.; Kambe, T.; Fujiwara, A.; Kubozono, Y. Characteristics of single crystal field-effect transistors with a new type of aromatic hydrocarbon, picene. *J. Phys. Chem. C* **2012**, *116*, 7983−7988.
(13) He, X.; Eguchi, R.; Goto, H.; Uesugi, E.; Hamao, S.; Takabayashi, Y.; Kubozono, Y. Fabrication of single crystal field-effect transistors with phenacene-type molecules and their excellent transistor characteristics. *Org. Electron.* **2013**, *14*, 1673−1682.
(14) He, X.; Hamao, S.; Eguchi, R.; Goto, H.; Yoshida, Y.; Saito, G.; Kubozono, Y. Systematic control of hole-injection barrier height with electron acceptors in [7]phenacene single-crystal field-effect transistors. *J. Phys. Chem. C* **2014**, *118*, 5284−5293.
(15) Kurihara, N.; Yao, A.; Sunagawa, M.; Ikeda, Y.; Terai, K.; Kondo, H.; Saito, M.; Ikeda, H.; Nakamura, H. High-Mobility Organic Thin-Film Transistors Over 10 cm2V-1s-1Fabricated Using Bis(benzothieno)naphthalene Polycrystalline Films. *Jpn. J. Appl. Phys.* **2013**, *52*, 05DC11.
(16) Okamoto, H.; Hamao, S.; Goto, H.; Sakai, Y.; Izumi, M.; Gohda, S.; Kubozono, Y.; Eguchi, R. Transistor application of alkyl-substituted picene. *Sci. Rep.* **2014**, *4*, 5048.
(17) Fan, H.; Zou, S.; Gao, J.; Chen, R.; Ma, Q.; Ma, W.; Zhang, H.; Chen, G.; Huo, X.; Liu, Z.; Dang, Y.; Hu, W. High-mobility organic single-crystalline transistors with anisotropic transport based on high symmetrical "H"-shaped heteroarene derivatives. *J. Mater. Chem. C* **2020**, *8*, 11477−11484.
(18) Shimo, Y.; Mikami, T.; Murakami, H. T.; Hamao, S.; Goto, H.; Okamoto, H.; Gohda, S.; Sato, K.; Cassinese, A.; Hayashi, Y.; Kubozono, Y. Transistors fabricated using the single crystals of [8]phenacene. *J. Mater. Chem. C* **2015**, *3*, 7370−7378.
(19) Okamoto, H.; Eguchi, R.; Hamao, S.; Goto, H.; Gotoh, K.; Sakai, Y.; Izumi, M.; Takaguchi, Y.; Gohda, S.; Kubozono, Y. An extended phenacene-type molecule, [8]phenacene: Synthesis and transistor application. *Sci. Rep.* **2014**, *4*, 5330.
(20) Shimo, Y.; Mikami, T.; Hamao, S.; Goto, H.; Okamoto, H.; Eguchi, R.; Gohda, S.; Hayashi, Y.; Kubozono, Y. Synthesis and transistor application of the extremely extended phenacene molecule, [9]Phenacene. *Sci. Rep.* **2016**, *6*, 21008.
(21) Okamoto, H.; Kawasaki, N.; Kaji, Y.; Kubozono, Y.; Fujiwara, A.; Yamaji, M. Air-assisted high-performance field-effect transistor with thin films of picene. *J. Am. Chem. Soc.* **2008**, *130*, 10470−10471.
(22) Kawasaki, N.; Kubozono, Y.; Okamoto, H.; Fujiwara, A.; Yamaji, M. Trap states and transport characteristics in picene thin film field-effect transistor. *Appl. Phys. Lett.* **2009**, *94*, 043310.
(23) Kaji, Y.; Ogawa, K.; Eguchi, R.; Goto, H.; Sugawara, Y.; Kambe, T.; Akaike, K.; Gohda, S.; Fujiwara, A.; Kubozono, Y. Characteristics of conjugated hydrocarbon based thin film transistor with ionic liquid gate dielectric. *Org. Electron.* **2011**, *12*, 2076−2083.
(24) Sugawara, Y.; Ogawa, K.; Goto, H.; Oikawa, S.; Akaike, K.; Komura, N.; Eguchi, R.; Kaji, Y.; Gohda, S.; Kubozono, Y. O2-exposure and light-irradiation properties of picene thin film field-effect transistor: A new way toward O2 gas sensor. *Sens. Actuators, B* **2012**, *171−172*, 544−549.
(25) Komura, N.; Goto, H.; He, X.; Mitamura, H.; Eguchi, R.; Kaji, Y.; Okamoto, H.; Sugawara, Y.; Gohda, S.; Sato, K.; Kubozono, Y. Characteristics of [6]phenacene thin film field-effect transistor. *Appl. Phys. Lett.* **2012**, *101*, 083301.
(26) Kubozono, Y.; He, X.; Hamao, S.; Teranishi, K.; Goto, H.; Eguchi, R.; Kambe, T.; Gohda, S.; Nishihara, Y. Transistor application of phenacene molecules and their characteristics. *Eur. J. Inorg. Chem.* **2014**, 3806−3819.
(27) Okamoto, H.; Hamao, S.; Kozasa, K.; Wang, Y.; Kubozono, Y.; Pan, Y.-H.; Yen, Y.-H.; Hoffmann, G.; Tani, F.; Goto, K. Synthesis of [7]phenacene incorporating tetradecyl chains in the axis positions and its application in field-effect transistors. *J. Mater. Chem. C* **2020**, *8*, 7422−7435.
(28) Okamoto, H.; Hamao, S.; Eguchi, R.; Goto, H.; Takabayashi, Y.; Yen, P. Y.-H.; Liang, L. U.; Chou, C.-W.; Hoffmann, G.; Gohda, S.; Sugino, H.; Liao, Y.-F.; Ishii, H.; Kubozono, Y. Synthesis of the extended phenacene molecules, [10]phenacene and [11]phenacene, and their performance in a field-effect transistor. *Sci. Rep.* **2019**, *9*, 4009.
(29) Colinge, J.-P.; Colinge, C. A. *Physics of Semiconductor Devices*; Kluwer Academic Publishers: Boston, 2002; pp 165−250.

https://doi.org/10.1021/acsomega.1c06932
ACS Omega 2022, 7, 5495−5501